OPEN SCIENTIFIC LECTURES 2024

Spectrograms in frequency analysis of a chain of real mechanical oscillators subjected to creep-slip friction

Presenter: Paweł Olejnik

Department of Automation, Biomechanics, and Mechatronics K-11
Faculty of Mechanical Engineering of TUL
POLAND

12. March, 2024, 12:00, Room 2M334

1. Introduction

In this presentation, we will discuss a real mechatronic system consisting of coupled inertia oscillations affected by relatively high-frequency structural vibrations.

We will provide a mathematical description of this system.

We will explain the numerical method for creating a spectrogram of real vibrations.

To simulate the presence of a real excitation mechanism in structural vibrations, a vibration exciter in the form of an imbalanced rotor is integrated into the model system.

Since this type of unavoidable excitation can be observed in the operation of any real machine, it is important to note that even small amplitude and fast forcing can significantly impact the frictional response of the observed creep-slip motion.

1. Introduction

In the design, a structural vibration analysis is often conducted on specific areas of the machine. The discussed problems related to dynamics are frequently caused by dry and viscous friction, as well as rotating imbalances occurring in driving and braking systems, stabilizing platforms, miscellaneous turbine and pump solutions, and others.

The common factor among these different types of vibration is that the structure exhibits repetitive dynamical behavior, which impacts its physical properties, positioning accuracy, and more.

2. Modeling the Physical System

2.1. Components of the Machine

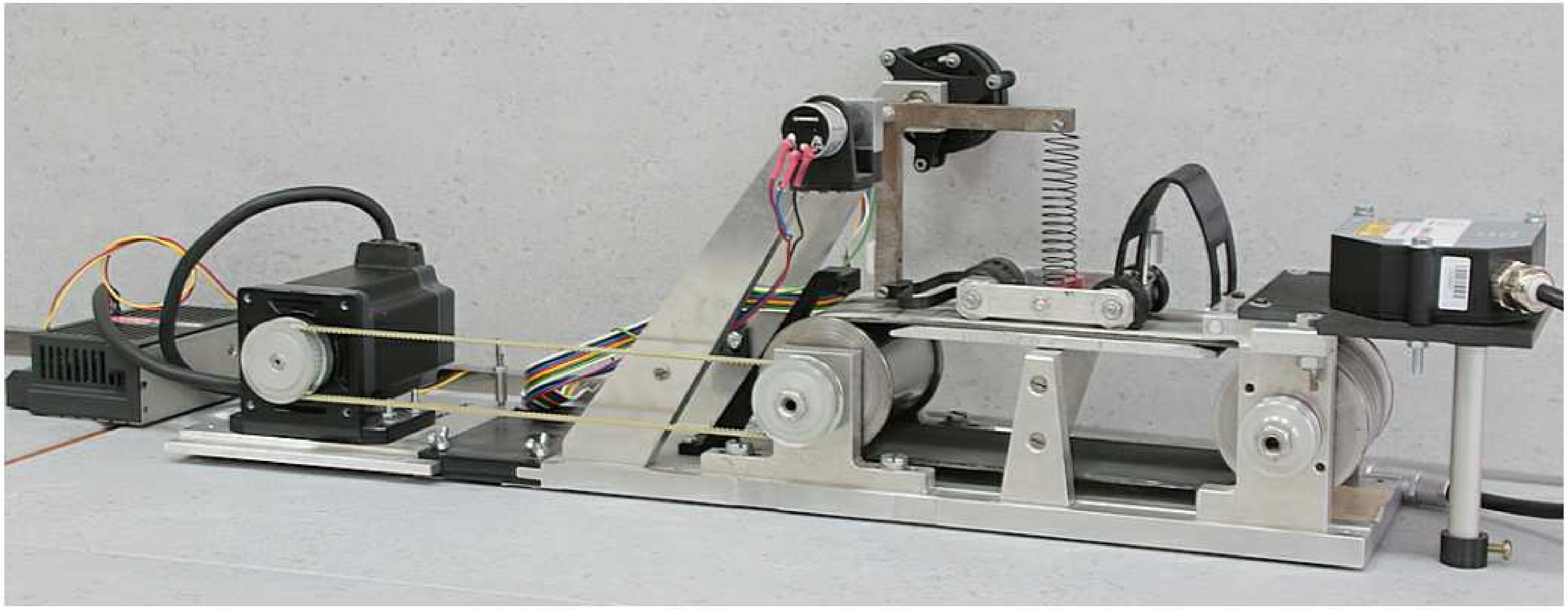

Figure 1. A real chain of oscillators with friction and soft elastic beams

2.2. The Mass Moment of Inertia of the Pendulum

$$J = m_a l^2 + J_s$$

$$J_s \approx m_a(b^2/4 + a^2/3 - ab/3)$$

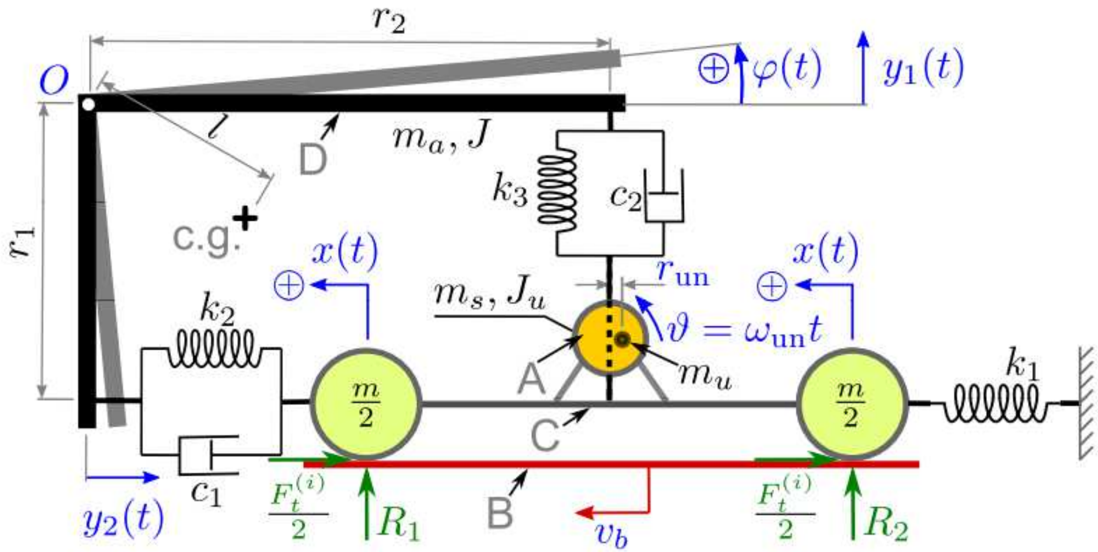

(a) chain of oscillators

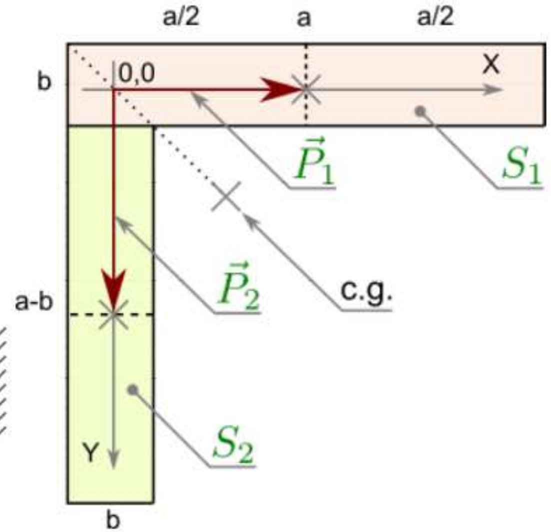

(b) pendulum

Figure 2. Physical model of the chain of oscillators J–m_u–m (a): A – imbalanced rotor mounted on C, see Figure 1, B – horizontally moving soft base, C – stiff beam in a contact at R_1 and R_2 with the base B, D – stiff non-symmetric pendulum body of mass moment of inertia J and mass m_a, see also (b), elasticity: k_1, k_2 k_3 and the viscous damping coefficients of spring couplings: c_1, c_2.

2.3. *The Imbalanced Rotor on the Sliding Block*

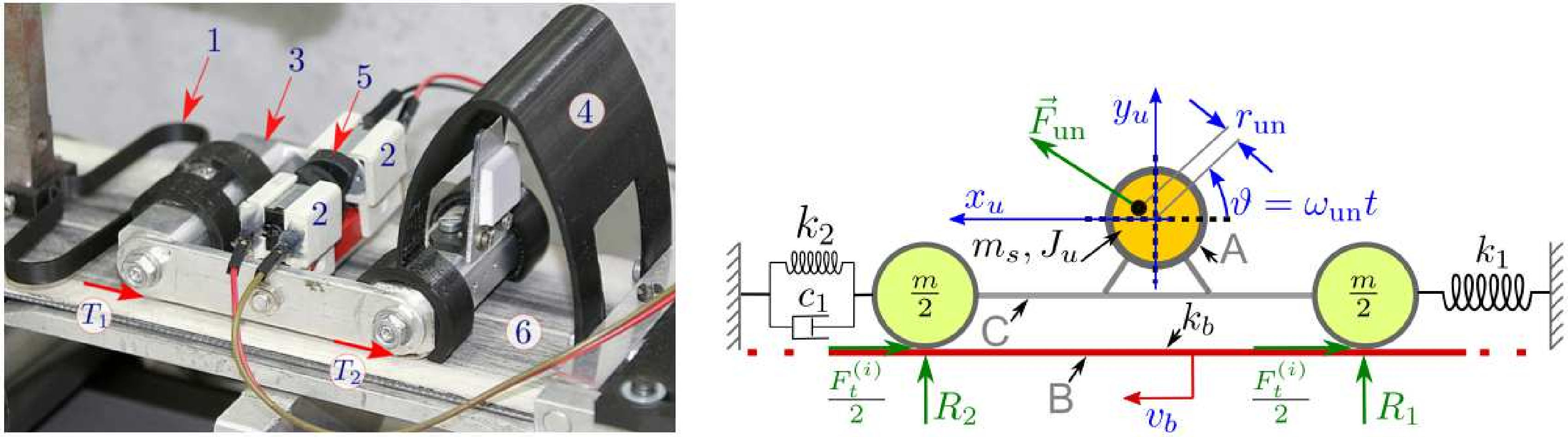

(a) rotor with an imbalance **(b)** the model

Figure 3. The sliding body (3) vibrating on the moving base (6) subjected to structural vibration induced by rotating imbalances (5) of the engines (2) with elastic reactions from belt springs (1 and 4). The base (6) moves precisely controlled with the use of a stepper motor while displacement of the oscillator is measured with the use of laser proximity switch (not visible on the right-hand side)

3. Mathematical Models of High-Frequency Excitation Forms of Structural Vibration

3.1. Varying High Frequency Forcing from a Driving System

3.2. Controlled High Frequency Forcing from an Unbalanced Rotor

3.3. Dynamical Model of the Pendulum-Block Coupling

Influence of Weak Structural Vibrations on a Machine-Driven Chain of Mechanical Oscillators with Friction under Varying Normal Forces

by Paweł Olejnik

Department of Automation, Biomechanics and Mechatronics, Faculty of Mechanical Engineering, Lodz University of Technology, 1/15 Stefanowski Str., 90-537 Lodz, Poland

Machines **2023**, *11*(7), 760; https://doi.org/10.3390/machines11070760

Submission received: 16 June 2023 / Revised: 9 July 2023 / Accepted: 17 July 2023 / Published: 21 July 2023

(This article belongs to the Section **Machines Testing and Maintenance**)

Experimenting on the laboratory test stand

5. Experimental Investigations and Time-Frequency Analysis

Initially, measurements were taken without excitation in the system, while maintaining the installed excitation subsystem to ensure consistent mass. The moving base speed was varied by adjusting the frequency input to the stepper motor. Four frequencies of the control signal applied

to the stepper motor's controller were selected for analysis: 1000, 3000, 10000 [steps/s] with a micro-step of 0.72/8 [deg]. The laser sensors of displacements of the linearly mowing block and the pendulum's arm operate at 2000 [readings/s].

Experimenting on the laboratory test stand

5.1. Controlling the Angular High Frequency of Excitation of the Moving Mass

The developed vibration excitation system represents a novel approach for inducing additional forcing to control the shape of self-excited or creep-slip vibrations. It involves a rotating disk with an off-center hole, causing a displacement of the center of gravity. The disk is mounted on the shafts of two small, synchronized DC motors positioned opposite each other. The system utilizes MT68 DC motors, capable of reaching a maximum speed of 12100 rpm (at no load), generating a torque of $0.21 \cdot 10^{-3}$ [N·m] and a power output of 0.2 [W].

Experimenting on the laboratory test stand

5.2. Time Histories in Monitoring of the Influence of the High-Frequency Structural Vibrations on the Stick-Slip Dynamical Response of the Self-Excited Block Oscillator

This section focuses on utilizing time histories to examine the effects of high-frequency structural vibrations on the stick-slip dynamics of a self-excited block oscillator. The oscillator is coupled in a chain with a pendulum, and the coupling is characterized by soft characteristics.

The observed phenomenon depicted in Figure 5 (black line) exhibits a periodically repeating sawtooth curve with an average amplitude of 1.223 [mm]. This behavior occurs when the slow base motion is applied without exciting the moving structure, represented by a solid body with mass M. This aligns with the theory of motion characteristics in frictional contact, where energy accumulates in the springs until the applied force reaches the threshold required for motion initiation. Once this force threshold is surpassed, the cart transitions from a state of rest to sliding, resulting in a descending slope of the curve that occurs at shorter time intervals. At this point, there should be an abrupt return of the object to its initial equilibrium position due to the accumulated energy.

Experimenting on the laboratory test stand

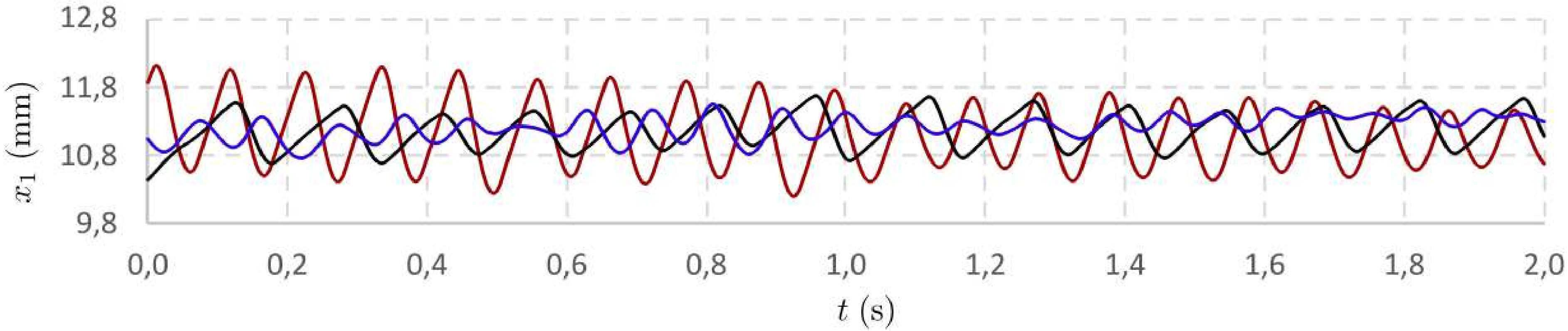

Figure 5. Real stick-slip trajectory of motion of the oscillator not subject to high-frequency external forcing at various base velocities: $v_b^{(\text{red})} = 3v_b^{(\text{black})}$ and $v_b^{(\text{blue})} = 10v_b^{(\text{black})}$

Experimenting on the laboratory test stand

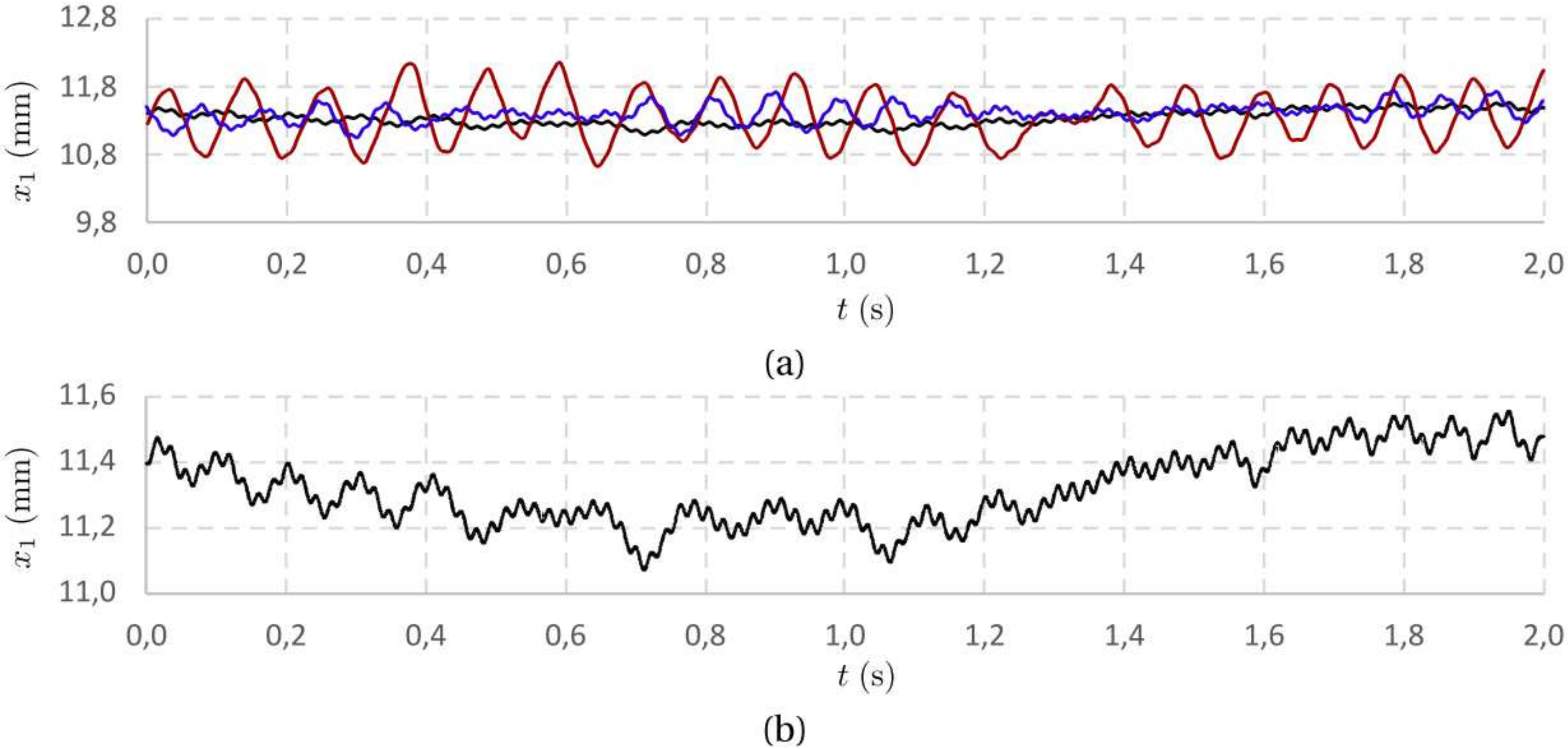

Figure 6. Real stick-slip trajectories of motion of the oscillator subject to high-frequency external forcing with high unbalancing (a) with zoomed black trajectory (b) at $\omega = 400$ [rad/s] and various base velocities: $v_b^{(red)} = 3v_b^{(black)}$ and $v_b^{(blue)} = 10v_b^{(black)}$

Experimenting on the laboratory test stand

5.3. Spectrograms in Monitoring of the Influence of Structural Vibrations

In the previous subsection, we demonstrated the recording and time-series measurement of high-frequency vibrations caused by high-amplitude vibrations of the exciters (the engine 2 in Figure 3). However, detecting vibrations in a coupled oscillator system when the overall vibrations are very small presents a challenge. To overcome this, we utilize a tested oscillator system with a pendulum having a soft elastic characteristic as the detector. Our objective is to capture time trajectories that contain a hidden high-frequency component for further analysis. We aim to demonstrate that the presence of an excited oscillator with friction, oscillating in a frictional contact, modifies the amplitude range of vibrations (with a slight expected reduction in this dynamic parameter) and decreases the dwell times at the attachment point. Our analysis employs spectrograms, frequency response spectra, and amplitude spectra in decibels.

Experimenting on the laboratory test stand

Table 1 provides the configuration parameters for the subsequent experiments conducted on the research setup.

Table 1. Configuration parameters of the experiments (a case of small amplitude unbalancing vibration)

Figure No.	Oscillator type	High frequency forcing	Motor control (square wave freq.)
8	J	no	constant
9	J	yes	
10	m	no	
11	m	yes	
12	J	no	decreasing linear sweep
13	J	yes	
14	m	no	
15	m	yes	

J – the angle body pendulum with friction; m – the self-excited oscillator with friction

Spectrogram – no high-frequency forcing of the soft pendulum

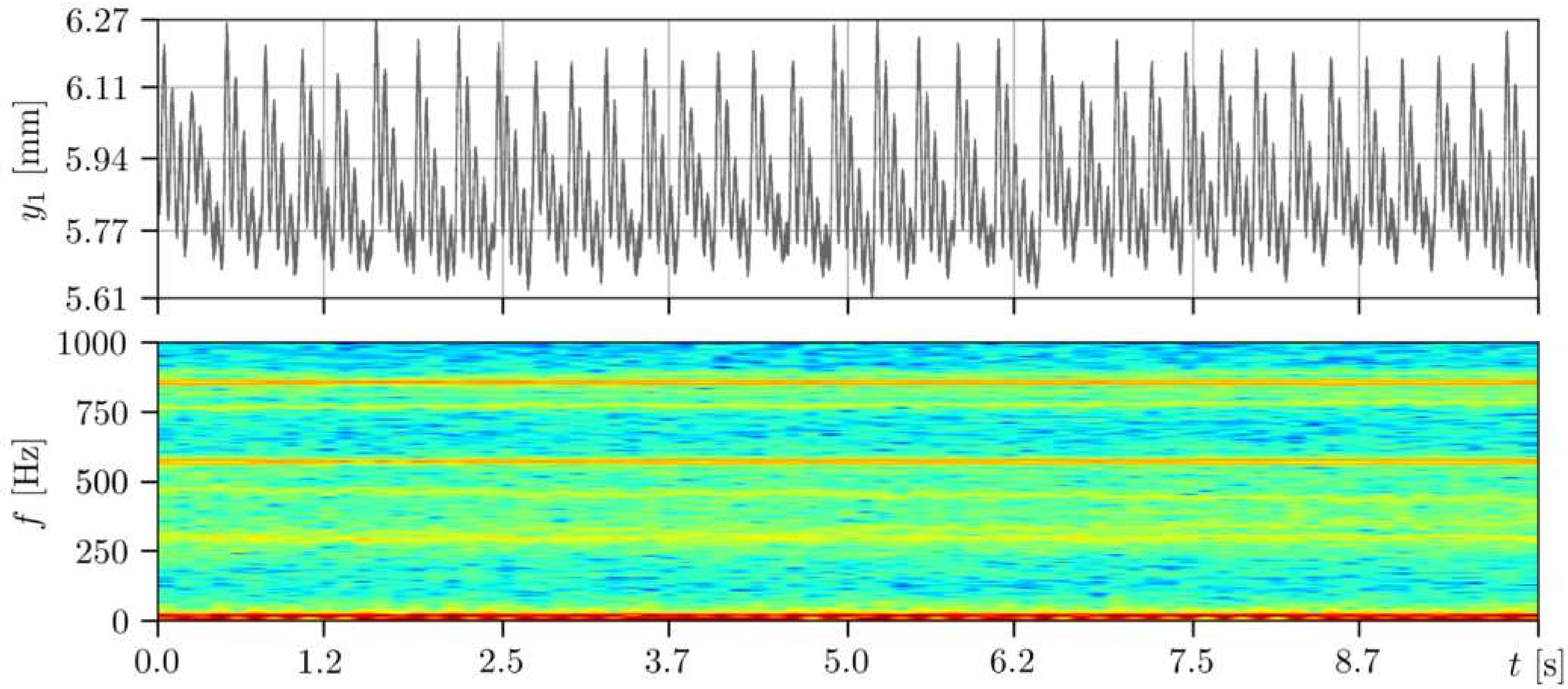

(a)

Figure 8. Time history, spectrogram, and magnitude plot of a coupled soft spring characteristic pendulum in the high (a, b) and low (c, d) frequency spectra. The base linear velocity is maintained at a constant of 7.2 [degrees/s], while the structure remains unaffected by high-frequency vibrations.

Spectrogram – with high-frequency forcing of the soft pendulum

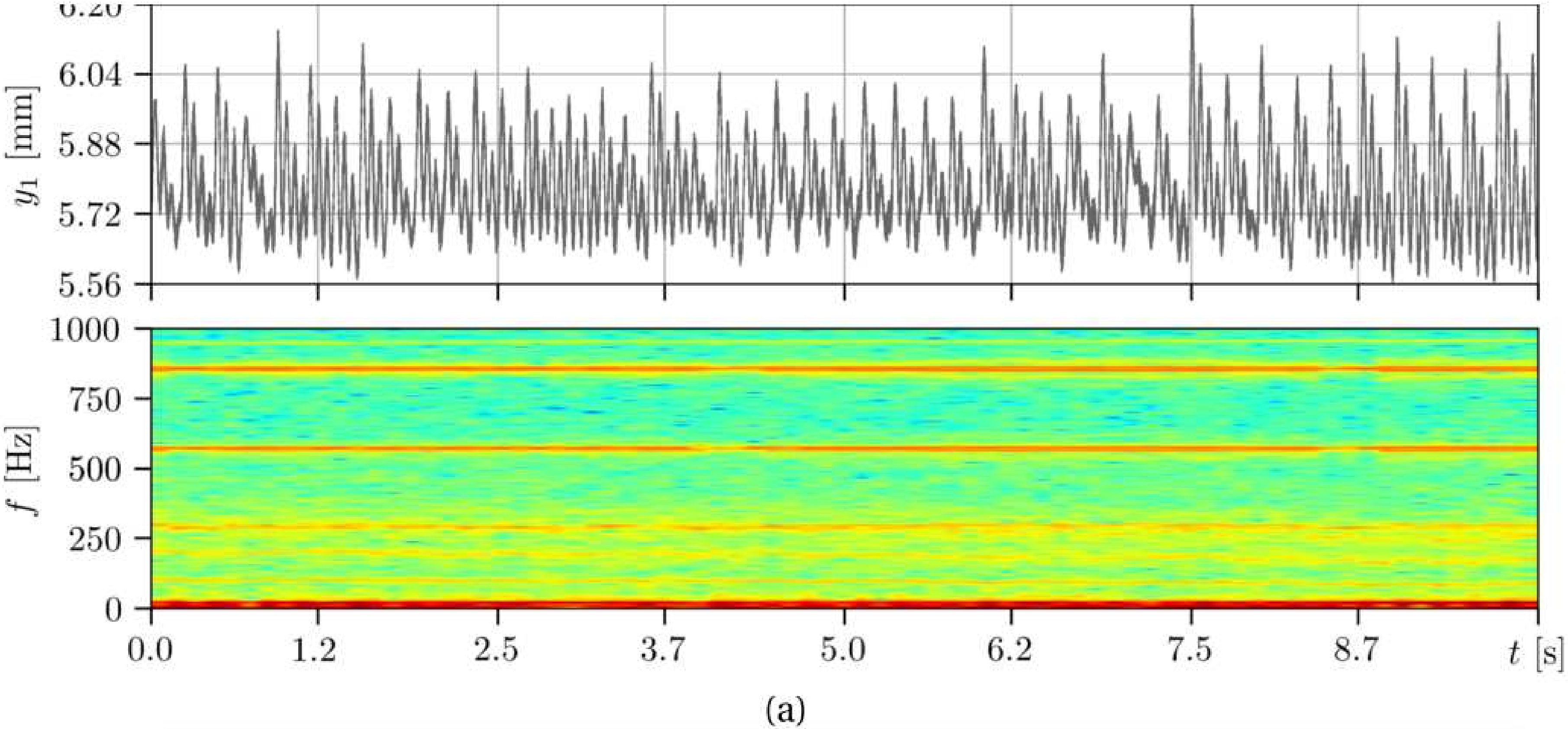

Figure 9. Time history, spectrogram, and magnitude plot of a coupled soft spring characteristic pendulum in the high (a, b) and low (c, d) frequency spectra. The base linear velocity is maintained at a constant of 7.2 [degrees/s]. The structure experiences high-frequency vibrations.

Spectral plots – no/with high-frequency forcing of the soft pendulum

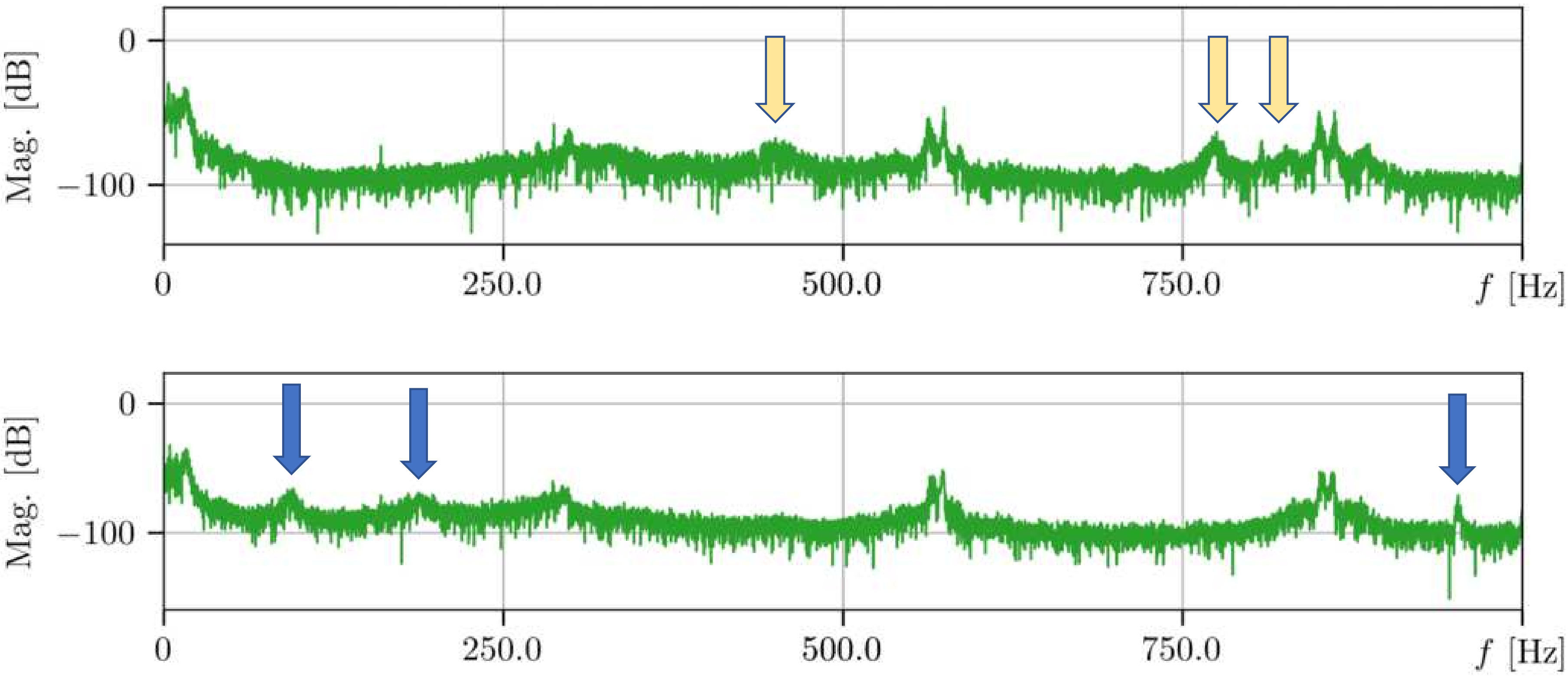

(b)

Spectrogram – no high-frequency forcing of the soft pendulum

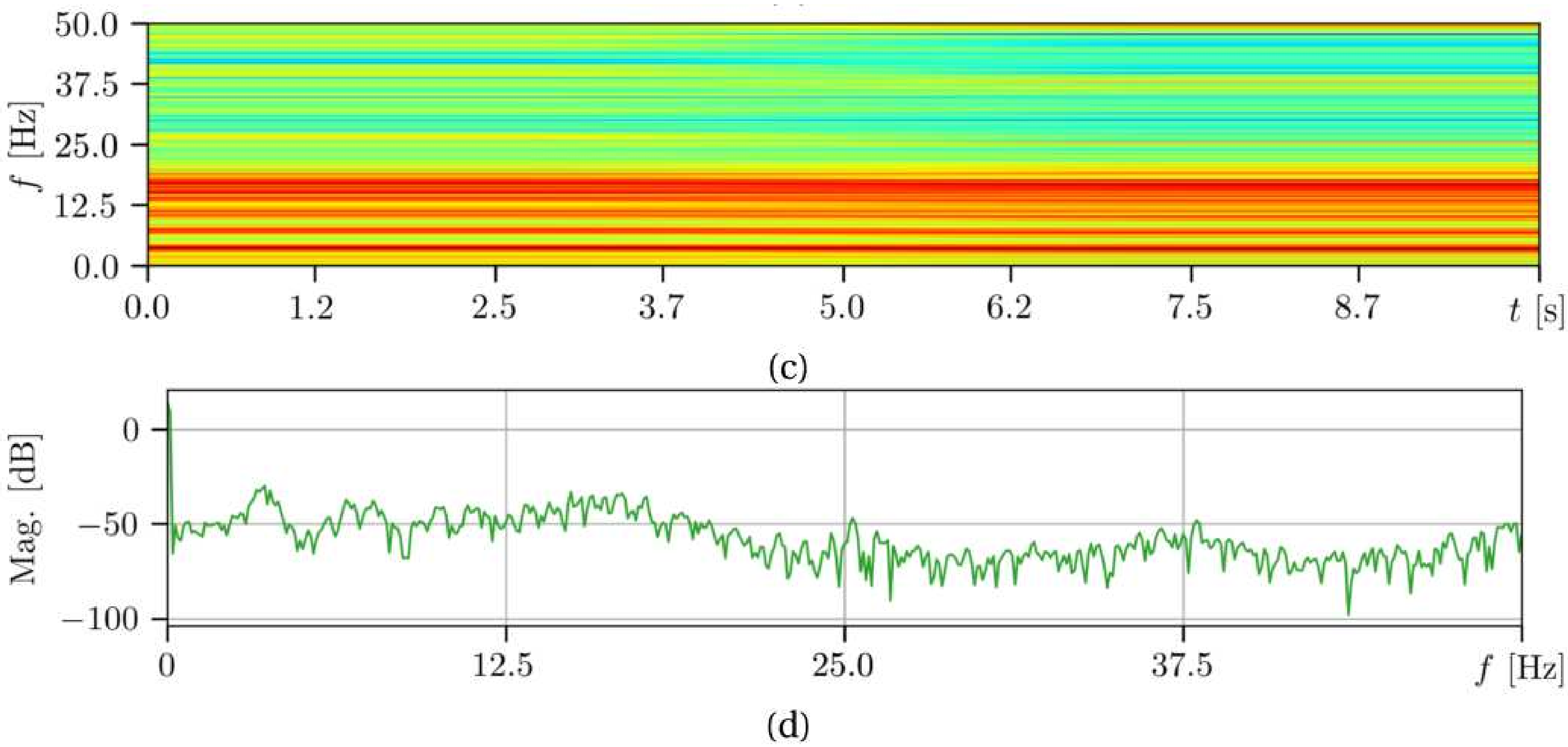

Figure 8. Time history, spectrogram, and magnitude plot of a coupled soft spring characteristic pendulum in the high (a, b) and low (c, d) frequency spectra. The base linear velocity is maintained at a constant of 7.2 [degrees/s], while the structure remains unaffected by high-frequency vibrations.

Spectrogram – <u>with</u> high-frequency forcing of the soft pendulum

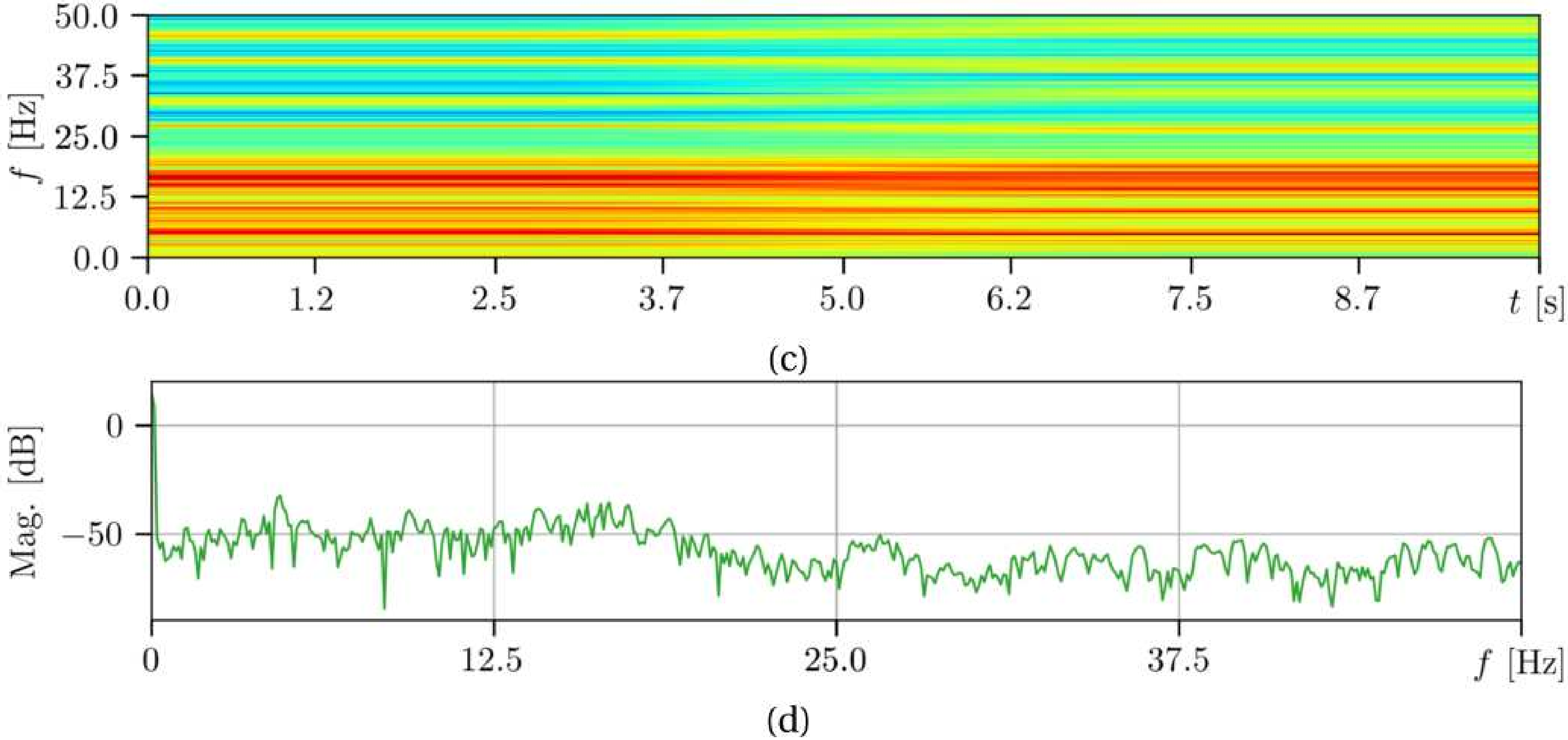

Figure 9. Time history, spectrogram, and magnitude plot of a coupled soft spring characteristic pendulum in the high (a, b) and low (c, d) frequency spectra. The base linear velocity is maintained at a constant of 7.2 [degrees/s]. The structure experiences high-frequency vibrations.

Spectrogram – no high-frequency forcing of the soft pendulum (slowly decreasing base velocity)

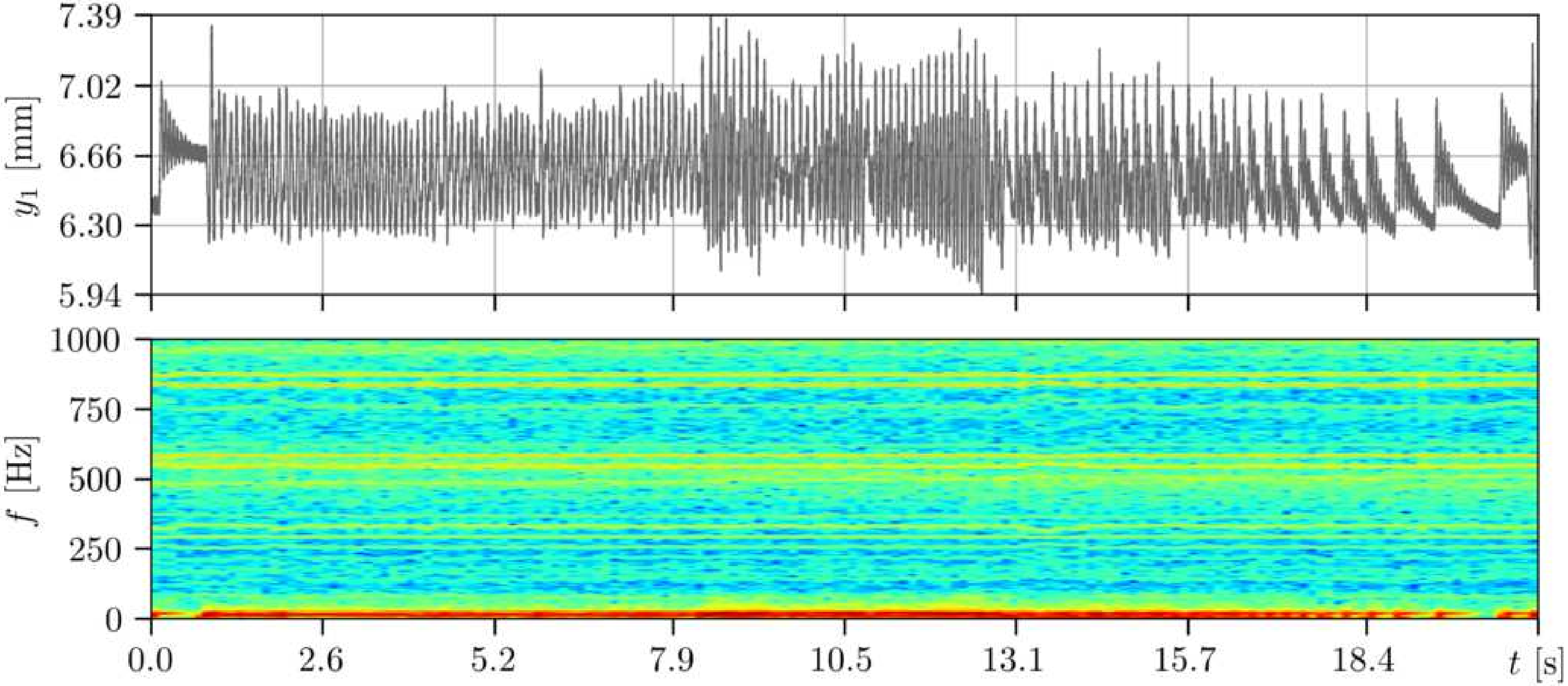

(a)

Figure 12. Time history, spectrogram, and magnitude plots illustrating the response of the pendulum dynamics to a sweep step wave driving the stepper motor. The base velocity decreases linearly from 7.2 [degrees/s] to 0 within a 20 [s] time frame, while high frequency forcing is not activated. The spectra are distinguished into high (up to 1000 [Hz]) and low (up to 50 [Hz]) frequency ranges.

Spectrogram – with high-frequency forcing of the soft pendulum (slowly decreasing base velocity)

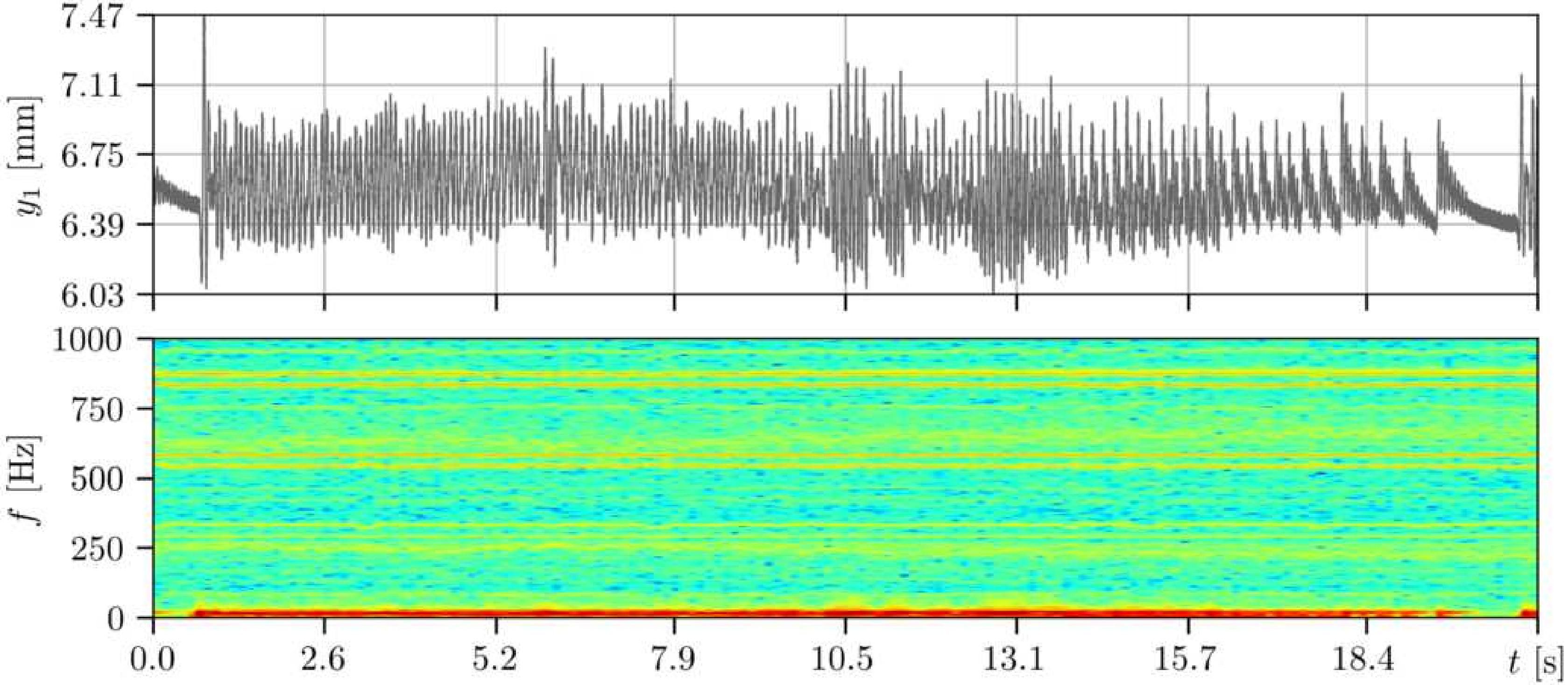

(a)

Figure 13. Time history, spectrogram, and magnitude plots illustrating the response of the pendulum dynamics to a sweep step wave driving the stepper motor. The base velocity decreases linearly from 7.2 [degrees/s] to 0 within a 20 [s] time frame, accompanied by the activation of high frequency forcing. The spectra are distinguished into high (up to 1000 [Hz]) and low (up to 50 [Hz]) frequency ranges.

Spectrogram – no high-frequency forcing of the soft pendulum at slowly decreasing base velocity

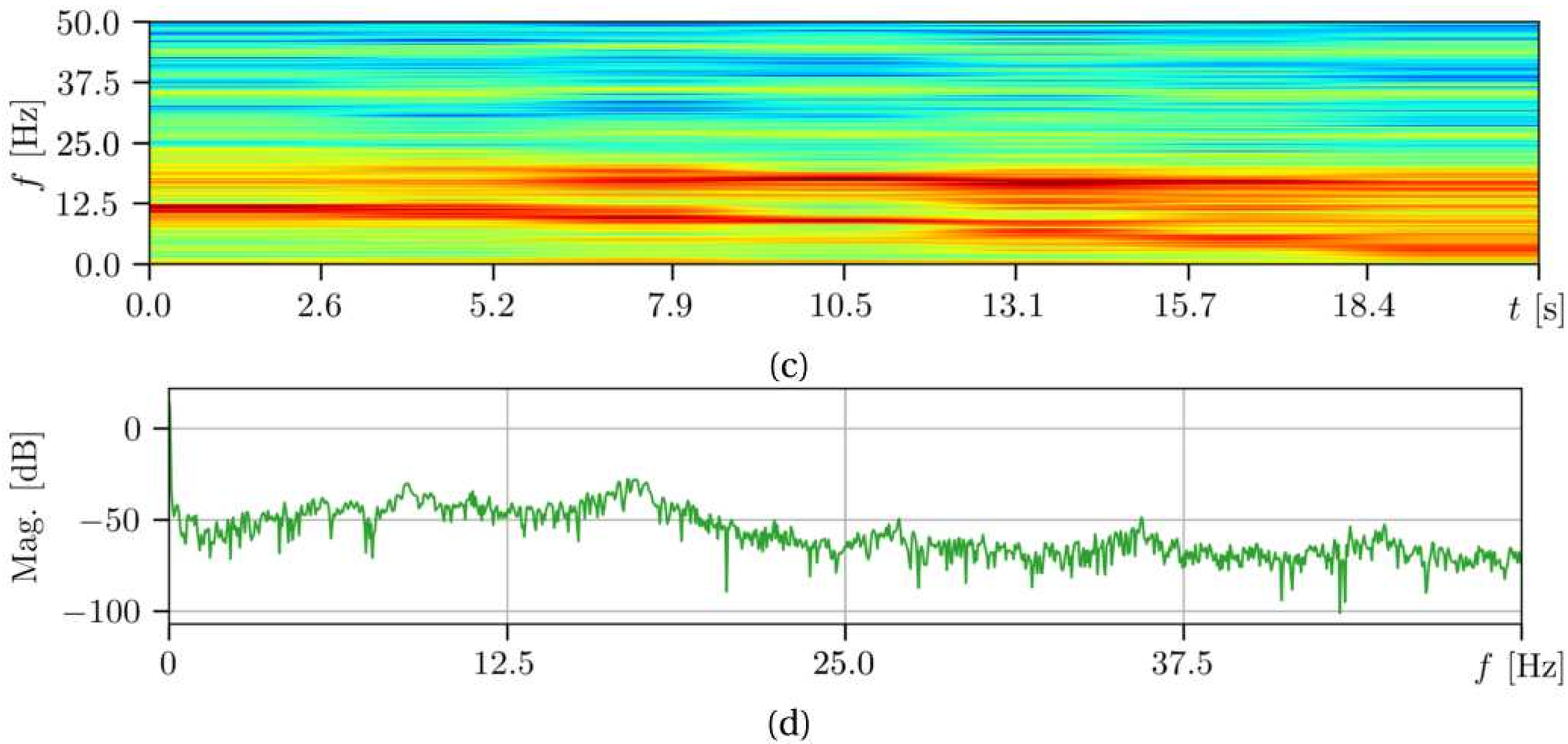

Figure 12. Time history, spectrogram, and magnitude plots illustrating the response of the pendulum dynamics to a sweep step wave driving the stepper motor. The base velocity decreases linearly from 7.2 [degrees/s] to 0 within a 20 [s] time frame, while high frequency forcing is not activated. The spectra are distinguished into high (up to 1000 [Hz]) and low (up to 50 [Hz]) frequency ranges.

Spectrogram – with high-frequency forcing of the soft pendulum at slowly decreasing base velocity

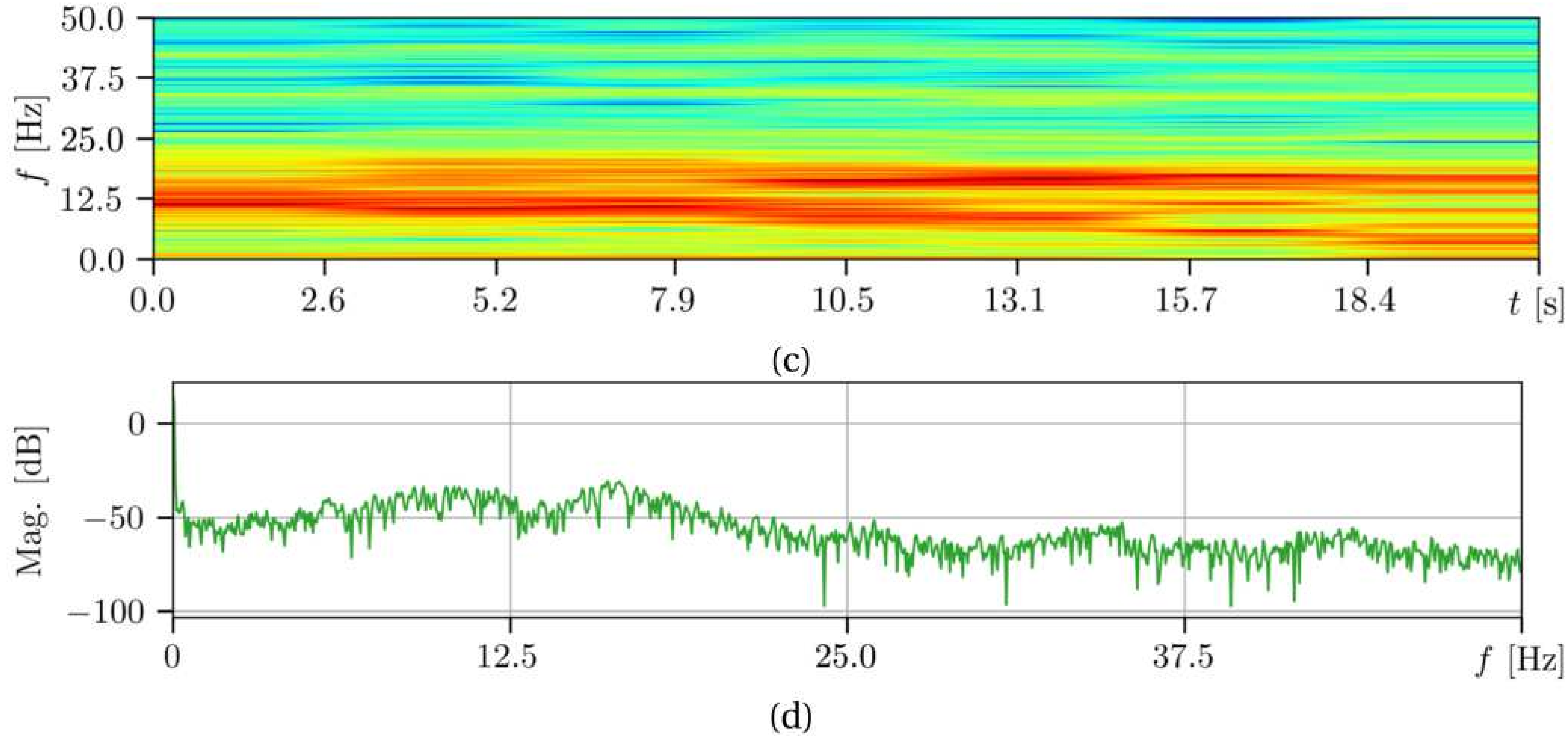

Figure 13. Time history, spectrogram, and magnitude plots illustrating the response of the pendulum dynamics to a sweep step wave driving the stepper motor. The base velocity decreases linearly from 7.2 [degrees/s] to 0 within a 20 [s] time frame, accompanied by the activation of high frequency forcing. The spectra are distinguished into high (up to 1000 [Hz]) and low (up to 50 [Hz]) frequency ranges.

Spectrogram – <u>no</u> high-frequency forcing of the self-excited oscillator

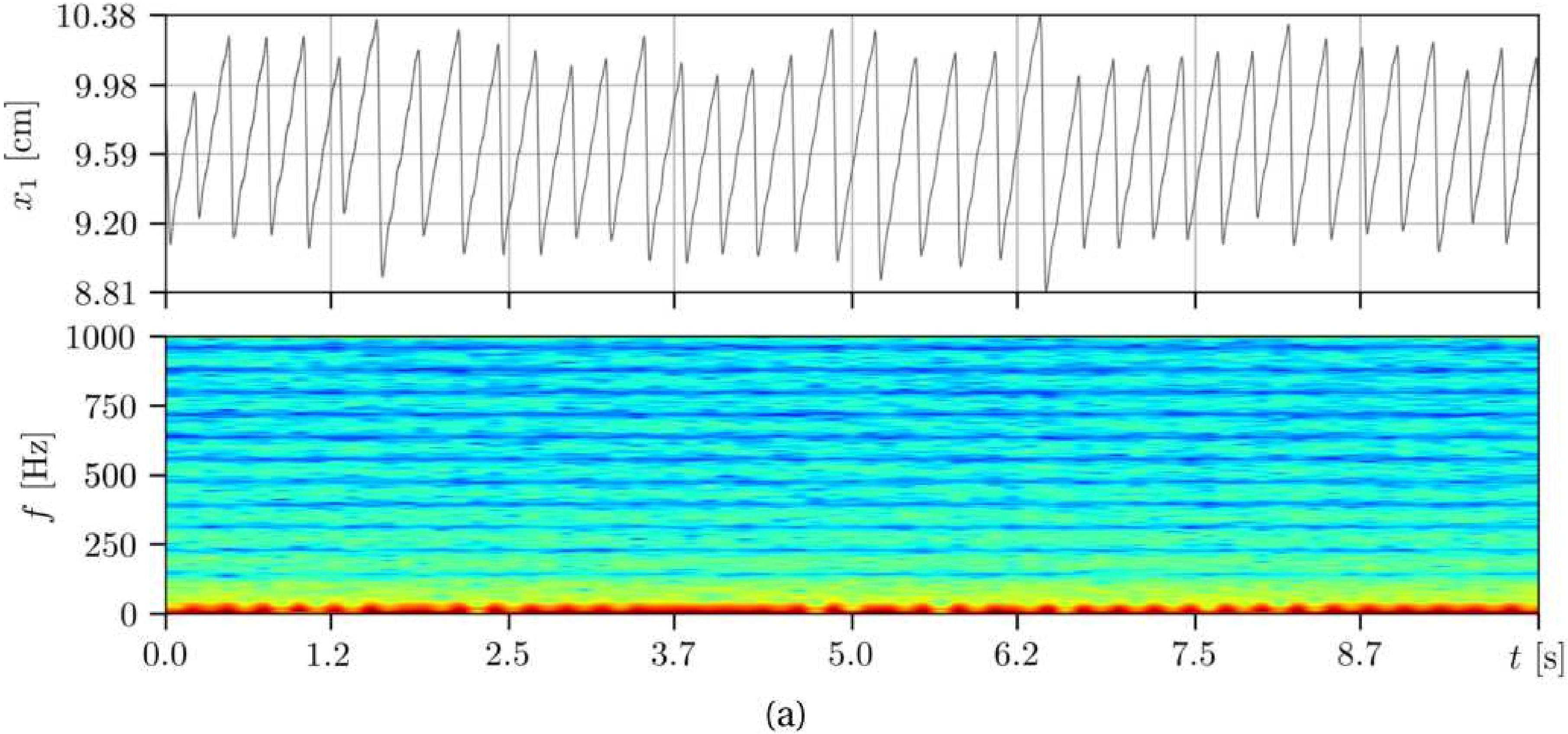

Figure 10. Time history, spectrogram, and magnitude plot of the self-excited block oscillator in the high (a, b) and low (c, d) frequency spectra. The base linear velocity is maintained at a constant of 7.2 [degrees/s], while the block remains unaffected by high-frequency vibrations.

Spectrogram – with high-frequency forcing of the self-excited oscillator

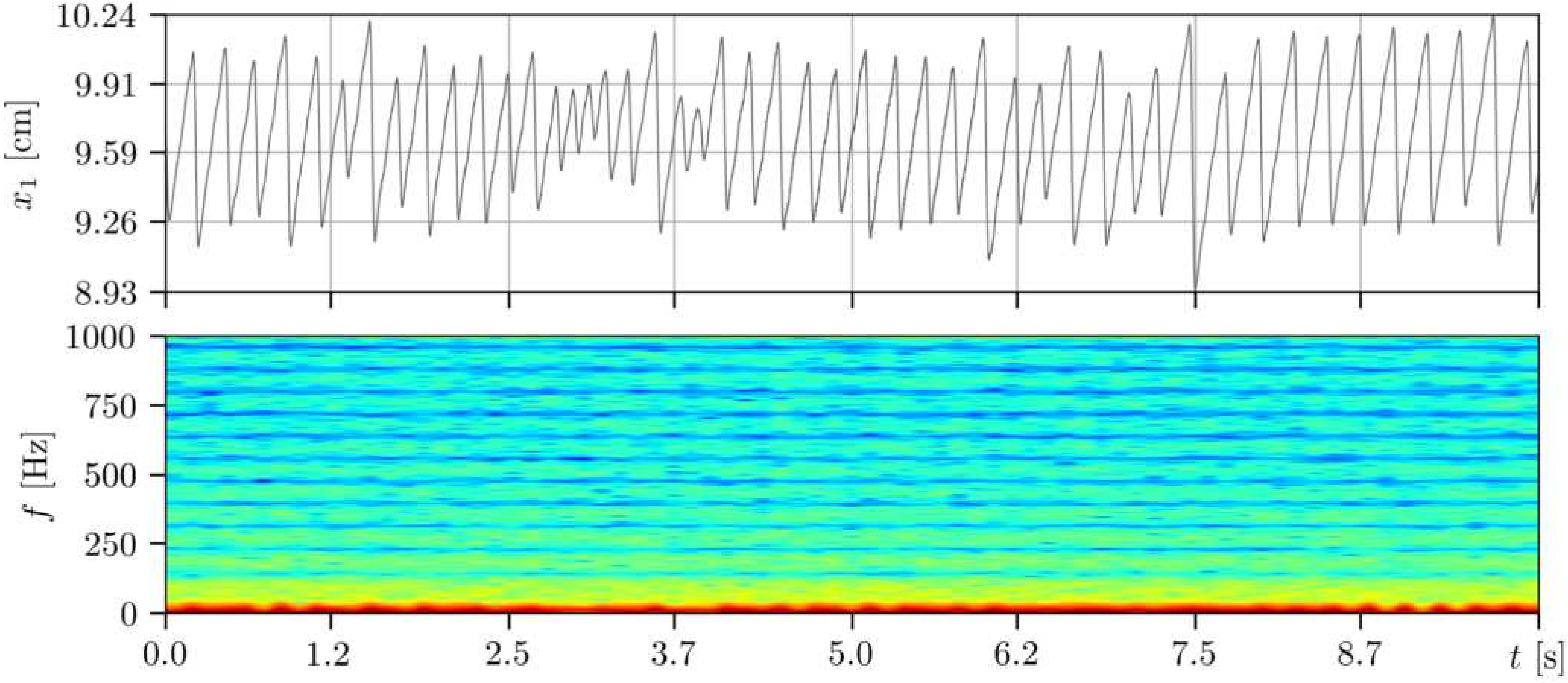

(a)

Figure 11. Time history, spectrogram, and magnitude plot of the self-excited block oscillator in the high (a, b) and low (c, d) frequency spectra. The base linear velocity remains constant at 7.2 [degrees/s], while the block undergoes high-frequency vibration.

Spectrogram – no high-frequency forcing of the self-excited oscillator

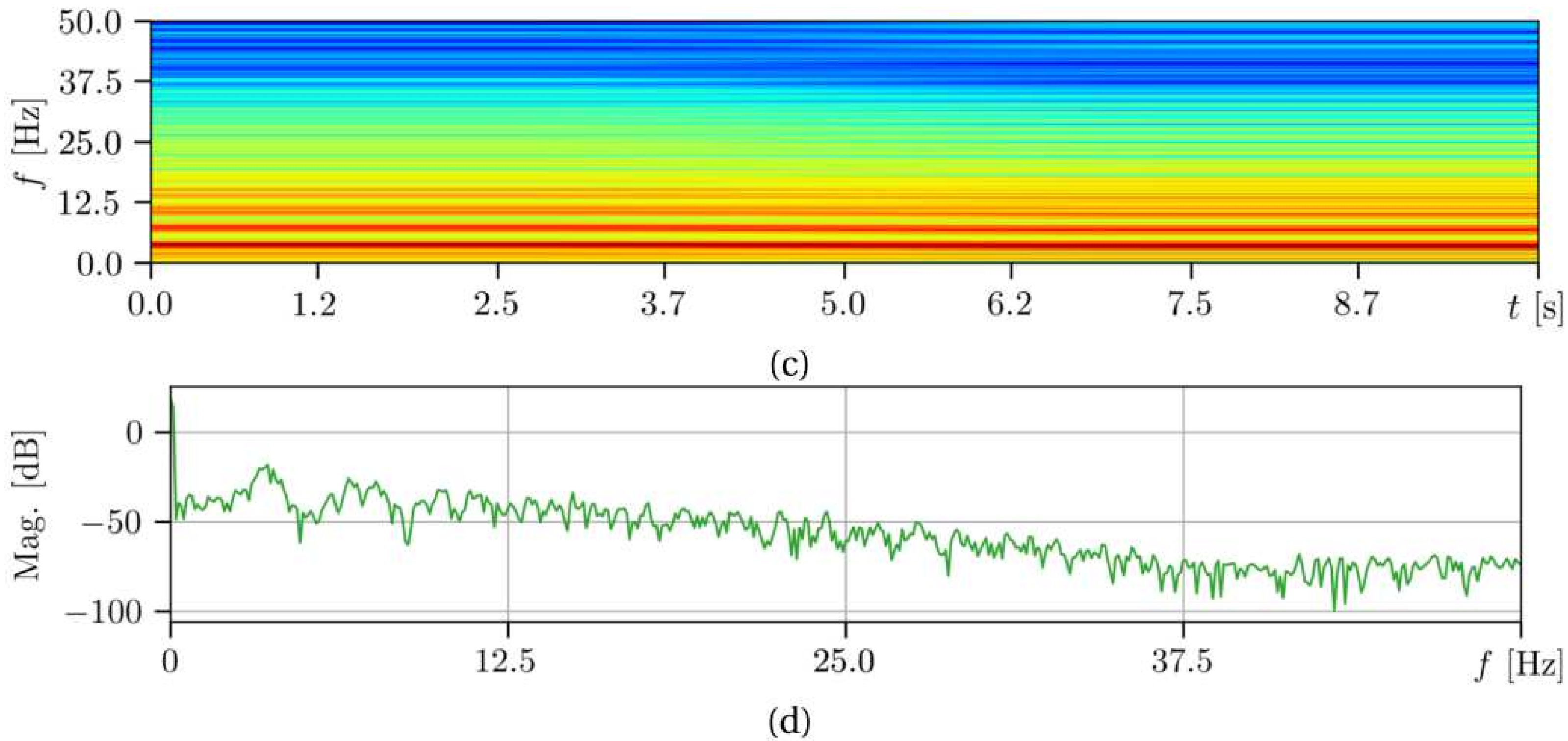

Figure 10. Time history, spectrogram, and magnitude plot of the self-excited block oscillator in the high (a, b) and low (c, d) frequency spectra. The base linear velocity is maintained at a constant of 7.2 [degrees/s], while the block remains unaffected by high-frequency vibrations.

Spectrogram – with high-frequency forcing of the self-excited oscillator

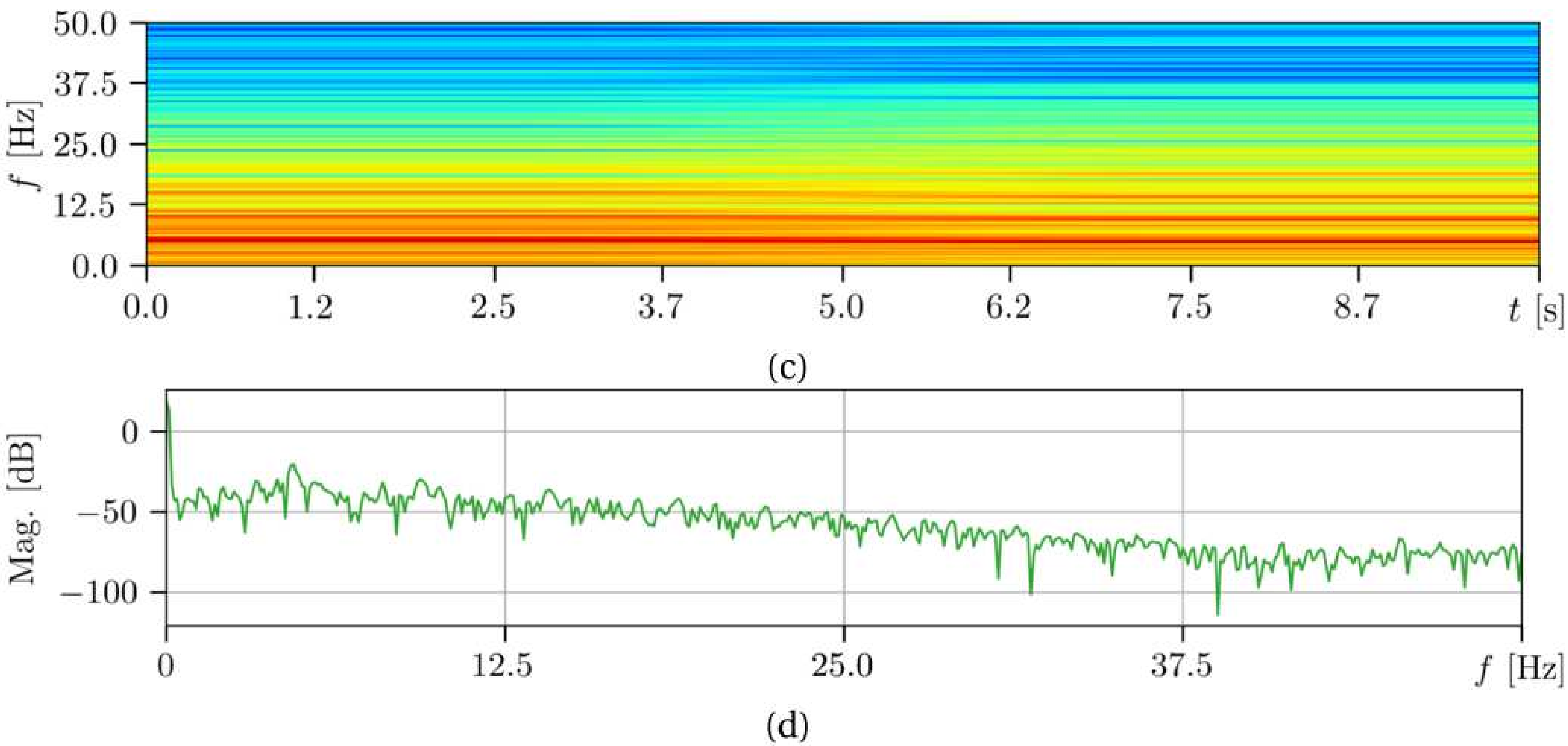

Figure 11. Time history, spectrogram, and magnitude plot of the self-excited block oscillator in the high (a, b) and low (c, d) frequency spectra. The base linear velocity remains constant at 7.2 [degrees/s], while the block undergoes high-frequency vibration.

Spectrogram – no high-frequency forcing of the self-excited oscillator at slowly decreasing base velocity

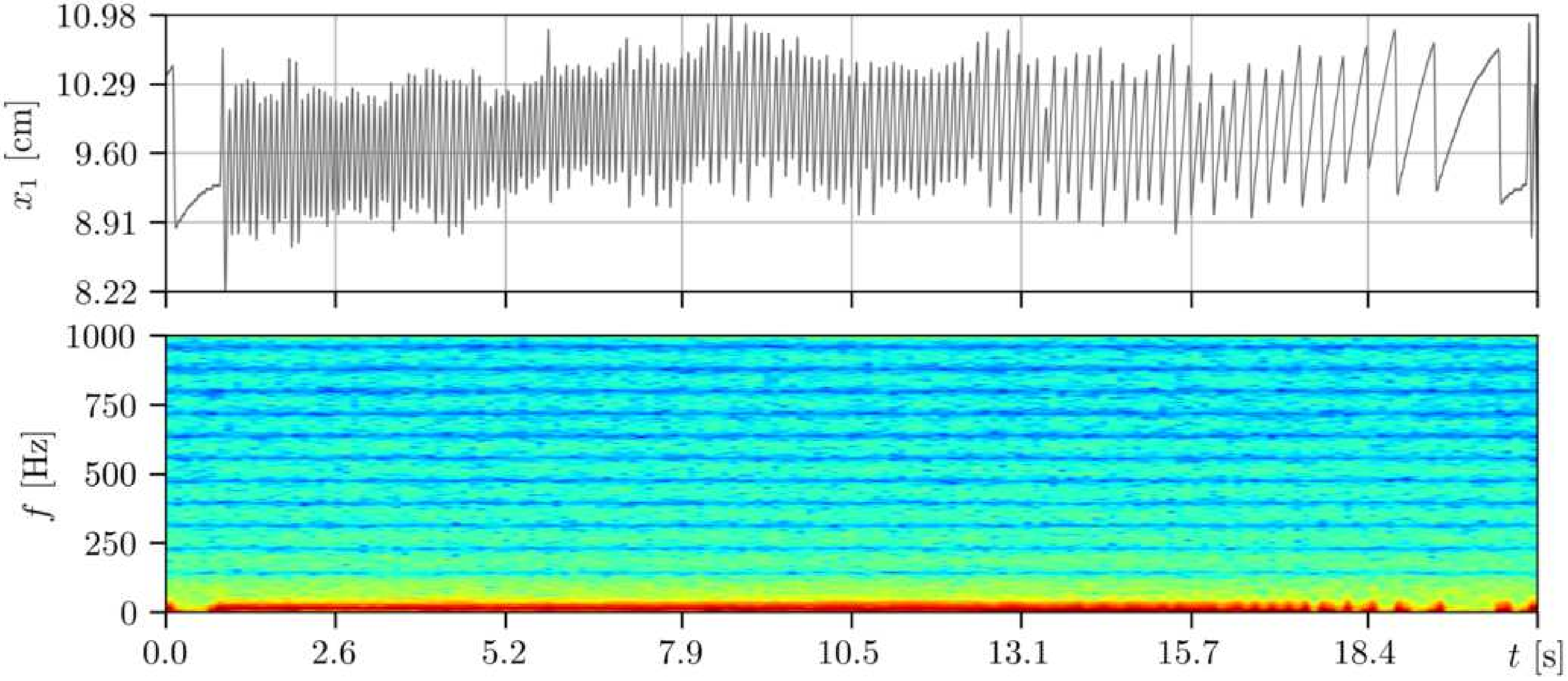

(a)

Figure 14. Time history, spectrogram, and magnitude plots illustrating the response of the self-excited block oscillator's dynamics to a sweep step wave driving the stepper motor. The base velocity decreases linearly from 7.2 [degrees/s] to 0 within a 20 [s] time frame, while high frequency forcing is not activated. The spectra are distinguished into high (up to 1000 [Hz]) and low (up to 50 [Hz]) frequency ranges.

Spectrogram – with high-frequency forcing of the self-excited oscillator at slowly decreasing base velocity

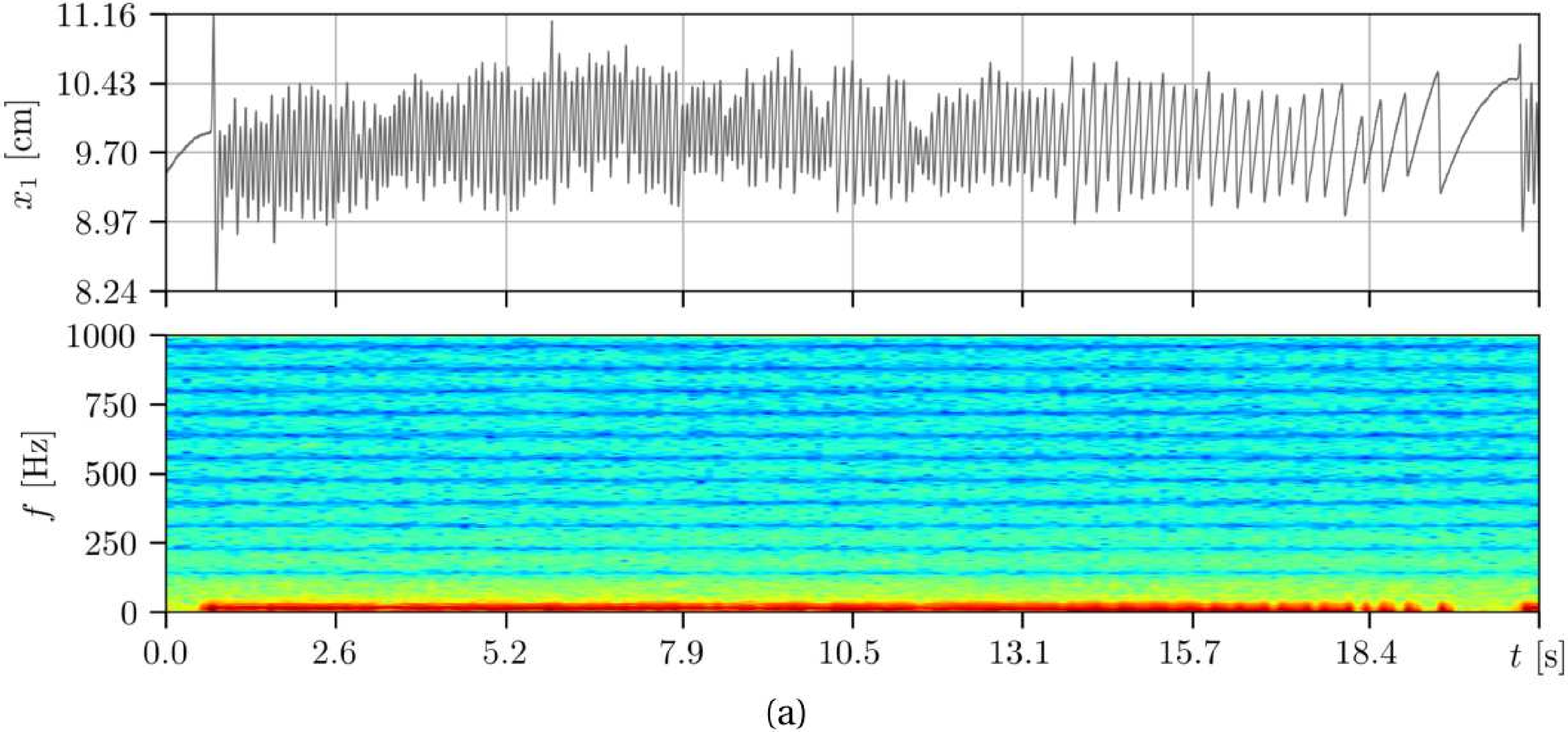

Figure 15. Time history, spectrogram, and magnitude plots illustrating the response of the self-excited block oscillator's dynamics to a sweep step wave driving the stepper motor. The base velocity decreases linearly from 7.2 [degrees/s] to 0 within a 20 [s] time frame, accompanied by the activation of high frequency forcing. The spectra are distinguished into high (up to 1000 [Hz]) and low (up to 50 [Hz]) frequency ranges.

Spectrogram – no high-frequency forcing of the self-excited oscillator at slowly decreasing base velocity

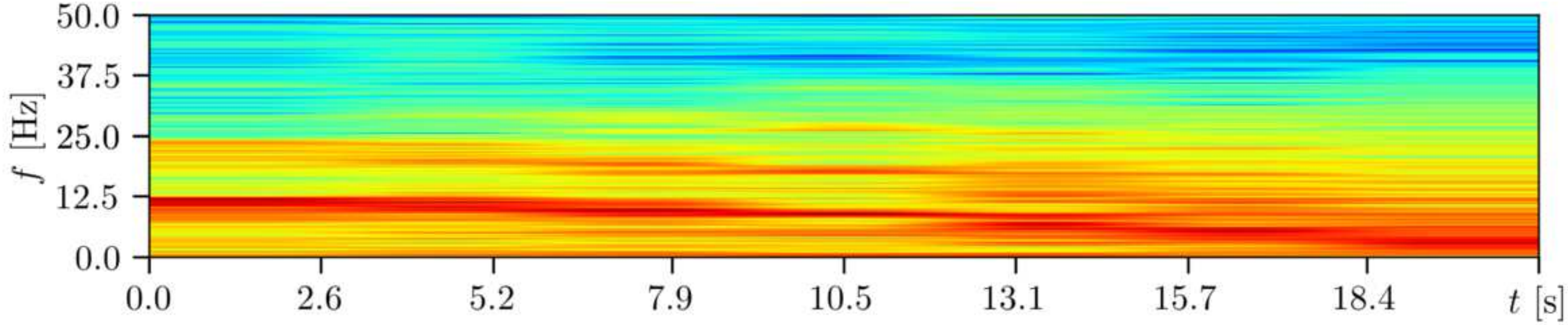

(c)

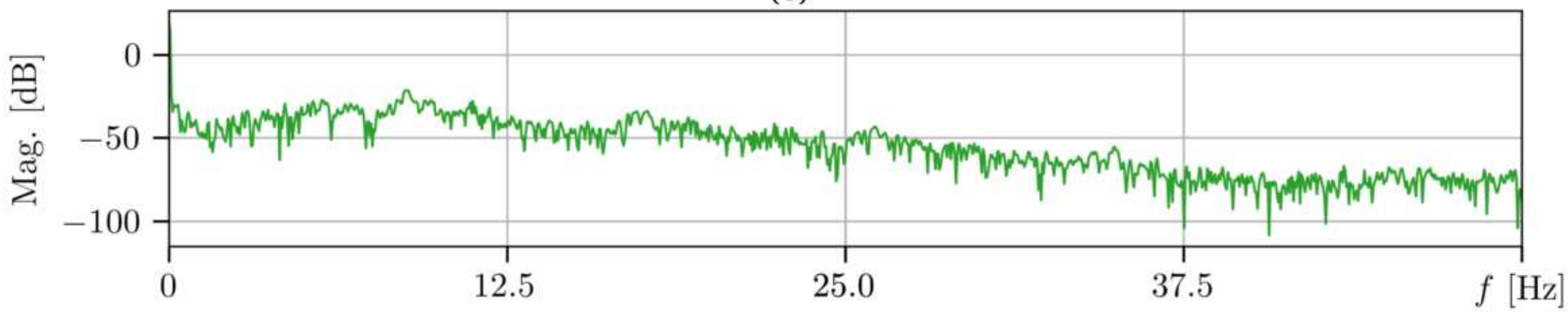

(d)

Figure 14. Time history, spectrogram, and magnitude plots illustrating the response of the self-excited block oscillator's dynamics to a sweep step wave driving the stepper motor. The base velocity decreases linearly from 7.2 [degrees/s] to 0 within a 20 [s] time frame, while high frequency forcing is not activated. The spectra are distinguished into high (up to 1000 [Hz]) and low (up to 50 [Hz]) frequency ranges.

Spectrogram – <u>with</u> high-frequency forcing of the self-excited oscillator at slowly decreasing base velocity

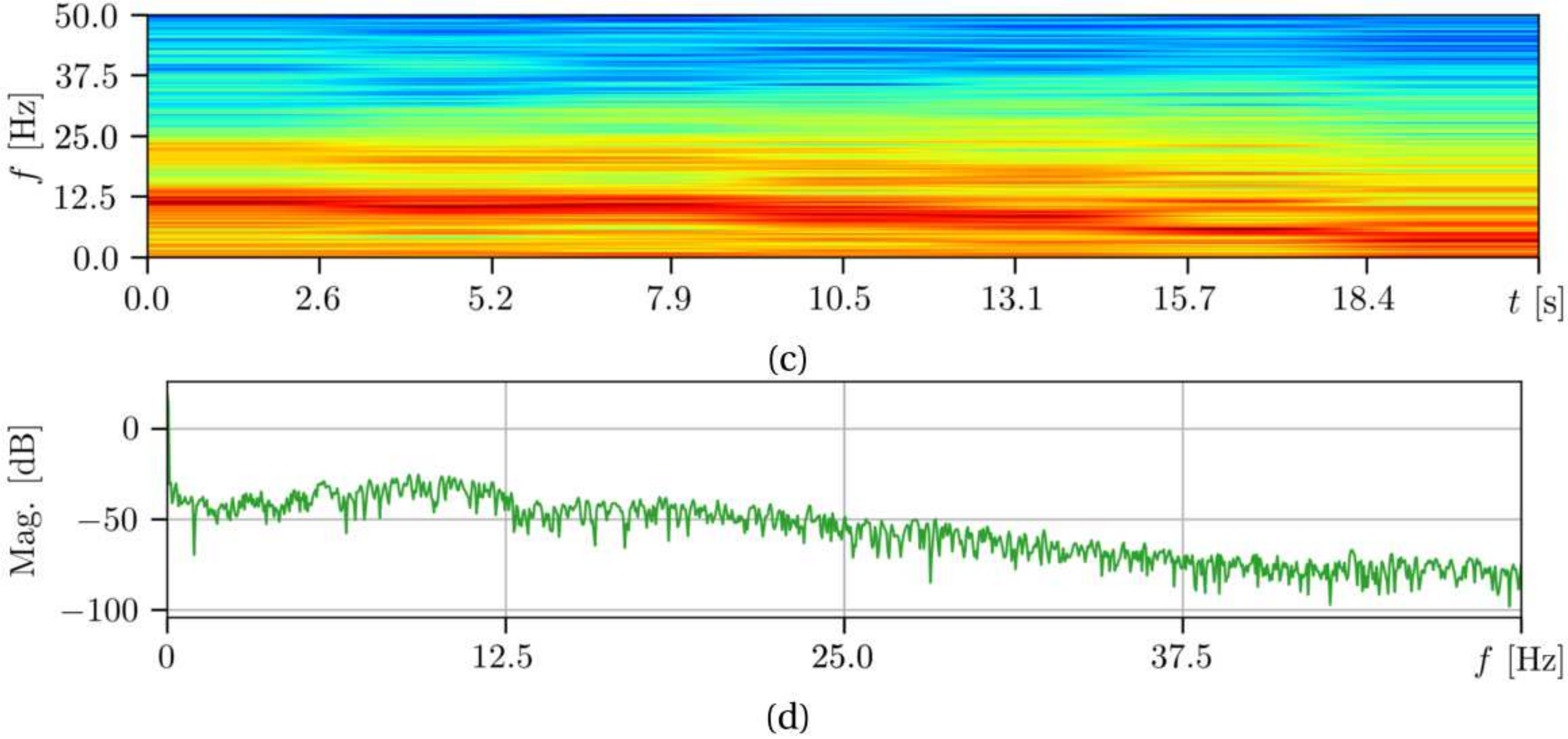

Figure 15. Time history, spectrogram, and magnitude plots illustrating the response of the self-excited block oscillator's dynamics to a sweep step wave driving the stepper motor. The base velocity decreases linearly from 7.2 [degrees/s] to 0 within a 20 [s] time frame, accompanied by the activation of high frequency forcing. The spectra are distinguished into high (up to 1000 [Hz]) and low (up to 50 [Hz]) frequency ranges.

Conclusions

The pendulum's solid body, while not directly influenced by the motors attached to the structure of the sliding block on the movable base, effectively captures these vibrations and serves as a means for their detection. This phenomenon was clearly observed in the spectrograms presented.

The impact of time-varying excitation on the dynamics of a 2-DoF mechanical system was investigated. Both models studied exhibit similar behavior and comparable changes in their dynamical characteristics. However, the influence of excitation frequency of the structure is clearly observable. The higher frequency modes generated by the motors, which induce structural vibrations, significantly affect the dynamics of the driven system.

Finally, experimental observations demonstrate that the nature of real mechanical contacts, experiencing sliding or creep-slip friction, undergoes changes when actual driving units are integrated into the machines. Including such a phenomenon in numerical modeling is very challenging to achieve. However, by making certain assumptions, it may be possible to incorporate other sources of high-frequency vibrations and introduce noisy, non-smooth signals of external excitation.

THANK YOU!